Indian Journal of Chemistry
Vol. 57A, January 2018, pp. 18-25

Enhanced photocatalytic activity of mesoporous nano titania decorated with zinc phthalocyanine

P V R K Ramacharyulu[a, b, *] & G K Prasad,[a, *]

[a]Defence R&D Establishment, Jhansi Road, Gwalior 474 002, MP, India
[b]National Dong Hwa University, Hualien 97401, Taiwan, ROC
Email: ramamsc2007@gmail.com/ gkprasad2001@gmail.com

Received 3 August 2017; re-revised and accepted 26 December 2017

Zinc phthalocyanine decorated mesoporous titania (Znpc-TiO_2), has been synthesized by a hydrothermal method, This visible light active nanocatalyst with a specific surface area of 247 m^2 g^{-1} degrades one of the highly toxic chemical warfare agents, sulfur mustard and malchite green dye photocatalytically in the sunlight with an exposure time of as low as 60 min.

Keywords: Photocatalysis, Degradation, Dye degradation, Visible light degradation, Detoxification, Nanoparticles, Sulfur mustard, Malchite green, Titania

Semiconductor mediated photocatalysis has been used for past several decades for air and water purification. Titanium oxide (TiO_2) is one of the most widely used photocatalyst among many semiconductors because of its good chemical stability, less toxicity, high photoactivity and economic viability. The major drawback is its large band gap (3.2 eV) which requires UV radiation (~388 nm) to activate it. However, only 4-5% in sunlight is UV and ~40% is visible light. To utilize visible light effectively by extending its spectral response towards longer wavelengths, several approaches have been implemented, i. e., metal doping, non-metal doping, dye sensitization, coupling with other semiconductors, and, defect induction in lattice.[1(a-d)]

Organic dye photosensitization, one of the approaches in which a dye adsorbed on TiO_2 surface gets excited by absorbing visible light, has proved to be an inexpensive and efficient method to widen the absorption spectra of TiO_2 into the visible light region.[2-5] This technique has been reported as an advanced technology which can play an significant role in developing effective and economic semiconductor photocatalyst system in the near future.[5] Several methods have been applied towards the visible light induced decontamination of pollutants. Dye sensitization mechanism initiates with electron injection from the excited dye into the conduction band (CB) of TiO_2, followed by interfacial electron transfer. The excited dyes interact with triplet ground molecular oxygen and generate singlet oxygen or superoxide radicals via an electron transfer pathway.[6, 7(a-b)] Being more oxidizing, the singlet oxygen reacts more readily with adsorbed pollutant molecules than triplet oxygen.[7(c)] Various toxic pollutants like phenols, its derivatives, pollutant dyes, pharmaceutical products and pesticides have been degraded by using dye sensitized photocatalysts which can utilize 50% of solar energy.[6-11]

Sulfur mustard (SM, bis(2-chloroethyl) sulfide, $C_4H_8S_2Cl_2$), a highly toxic chemical warfare agent (CWA) used in the World War II, acts as a vesicant and blister agent that alkylates DNA and rapidly effects erythema and edema upon exposure.[12] The toxicity of SM molecule can be lost by hydrolysis, oxidation, elimination and rearrangement reactions.[12-15] Various semiconductors such as TiO_2, ZnO, TiO_2-MnO_2, zirconium doped Zn-Ti oxides, metal doped TiO_2-SiO_2 catalysts, ferric oxide/graphite oxide composites and TiO_2 based composites, etc., have been used for the detoxification of SM.[11,13,14] Modified TiO_2 with enhanced photocatalytic activity under the visible light irradiation has been explored for detoxifying CWA into non-toxic products in ecological sunlight. The modified catalysts utilize a higher amount (46%) of visible light in addition to UV light (4–5%).[13,16-17] Other than TiO_2, sensitizers on various supports like zeolite Y, MCM-41, silica, and titania-silica have been explored for SM decomposition.[18] Recently, Ramacharyulu *et al.* studied photocatalytic decomposition of SM on Fepc-TiO_2 and observed complete SM degradation within 70 min.[19]

Malachite green is a water soluble dye, widely used to dye wool, silk, cotton, leather, etc. It is also used as food additive and medical disinfectant. However, it can cause carcinogenesis, mutagenesis, teratogenecity and

respiratory toxicity upon oral consumption.[20] Various studies on MG dye degradation on various materials have been reported.[21]

While several studies on degradation of the above two toxic compounds are available in literature, zinc phthalocyanine decorated TiO_2 (Znpc-TiO_2) has not been explored for the photocatalytic decomposition/ degradation of SM and MG dye. Herein, we report the sunlight driven photocatalytic degradation of SM to non-toxic compounds.

Materials and Methods

Zinc phthalocyanine and titanium tetraisopropoxide (TTIP) were procured from Acros organics, UK. Dichloromethane, ethanol, ethyl acetate and acetonitrile were obtained from E. Merck India Ltd. Malchite green dye was procured from Loba Chemie Pvt Ltd, India. SM of 99% purity was synthesized in our laboratory. *(Caution: SM is a very toxic agent; hence these experiments should be done under the guidance of trained personnel equipped with individual protective equipment only.)*

Synthesis and characterization of Znpc-TiO_2 catalyst

Znpc-TiO_2 nanocatalyst was prepared by sol-gel hydrolysis of titanium(IV) isopropoxide (TTIP) followed by hydrothermal treatment. Zinc phthalocyanine (1 mol%) was dissolved in a minimum amount of dichloromethane and added to 50 mL anhydrous ethanol and 50 mL distilled water. TTIP (9 mL) was dissolved in 41 mL anhydrous ethanol separately. TTIP solution was added dropwise to the mixture of zinc phthalocyanine solution in ethanol and distilled water under vigorous stirring at room temperature. The obtained precipitate was transferred into a Teflon lined autoclave and heated at 80 °C for 24 h. The obtained solid was washed with excess ethanol in order to minimize hydrogen bonding, dried at room temperature and labelled as 1.0 Znpc-TiO_2. A similar procedure was adopted for preparing undoped nano TiO_2 for comparative studies and labelled as HT.

X-ray diffraction patterns were obtained using a Rigaku Ultima IV with Cu-Kα radiation source (λ = 0.15405 nm) with a scanning speed of 5°/ min in the 2θ range of 20° to 80°. Transmission electron microscopy (TEM) measurements were made on a TECNAI G^2S (FEI) transmission electron microscope. Samples were suspended in 30 mL acetone, and the suspension was sonicated for 30 min. After that, suspension was placed on carbon coated copper grids of 3 mm dia. and dried at room temperature prior to the analysis.

N_2 sorption isotherm was recorded at 77 K using Autosorb-iQ (Quantachrome Instuments). The samples were degassed at 120 °C for 6 h prior to analysis. Specific surface area was calculated by applying BET model within pressure range of P/P_0 of 0.05-0.30. The pore size distribution (PSD) was calculated by DFT method. The pore volume was calculated from the uptake at a relative pressure of 0.99 cc g^{-1}. UV-visible spectrum was recorded on a Shimadzu UV-1800 instrument. GC (Nucon Engineers, India) equipped with a FID detector, BP5 (30 m length, 0.5 mm i.d.), OV 17 (1 m length, 3 mm i.d.) columns, and GC equipped with FPD detector and BPX5 column (30 m length, 0.25 mm i.d.) of Thermo Fischer Scientific Corporation, Italy were used to monitor decontamination kinetics of SM and the formation of reaction products. GC-MS system (5973 Turbo, Agilent, USA) was used for characterization of the reaction products. FT-IR was recorded on a Perkin Elmer, USA instrument with KBr pellet samples in the range of 400–4000 cm^{-1}.

Photocatalytic degradation of sulfur mustard (SM)

The nanocatalyst (100 mg of Znpc-TiO_2 or HT) was taken in a quartz tube and 100 µL of dichloromethane solution containing 2 µL of SM was spiked on it. Then the dichloromethane was allowed to evaporate. Subsequently, the quartz tube containing the nanocatalyst was irradiated with sunlight. Intensity of light was measured by a digital light meter (model SLM 110, AW Sperry Instruments, USA) with the help of the adapters provided. Value of irradiance of sunlight was determined to be 95 mW/cm^2. All the experiments were carried out at room temperature (30±2 °C). The remaining SM was extracted with acetonitrile on periodic time intervals. The extracted samples were analyzed with GC affixed with FID detector to monitor the amount of degraded SM. Further, the solution was concentrated to 1 mL and analyzed for the major degradation products by GC-MS (model 5975B and 6890N).

Photocatalytic degradation of malchite green

A stock solution of malachite green of 0.1371×10^{-3} M (50 ppm) concentration was prepared by dissolving 0.050 g of malachite green in 1000 mL of doubly distilled water. The absorption maximum of the dye

was determined with the help of a spectrophotometer (Shimadzu model 106). Photocatalytic degradation of malachite green was studied by taking 5 mL reaction mixture (which contains 0.1 mM of malachite green and 0.025 g of Znpc-TiO_2) in a test tube and stirred in dark for 30 min to attain adsorption-desorption equillibrium. The dye solution containing photocatalyst was exposed to natural sunlight. At regular time intervals, sample was extracted and centrifuged and the supernatant was analyzed for the amount of dye remaining/degraded.

Results and Discussion

Characterization of the TiO_2 nanocatalysts

The as-synthesized Znpc-TiO_2 and TiO_2 nanocatalysts were characterized by XRD. XRD pattern depicts the peaks at 2θ values of 25.2°, 37.8°, 48.0°, 53.8°, 62.7°, 69.4.° and 75.3°, which are ascribed to anatase phase of TiO_2 with (101), (004), (200), (105), (204), (116) and (215) planes respectively (JCPDS card # 21-1272) (Fig. 1). In addition, a small peak at 30.7° is endorsed to the (110) plane of rutile phase. No peaks corresponding to brookite phase (another crystalline polymorph of TiO_2) or zinc phthalocyanine were observed in XRD. This synthesis procedure allows homogeneous distribution of Znpc on TiO_2 to form solid solution. The crystallite sizes of the synthesized nanocatalysts were calculated by Scherrer equation and found to vary between 6 and 10 nm. The crystallite size calculated from the XRD patterns is in good agreement with that estimated from TEM studies. The SEM and TEM images of Znpc-TiO_2 nanocatalyst indicate the particles of spherical shape with sizes in the range of 5-10 nm. Mostly these were in the agglomerated form. EDX data depicts the presence of Zn in the synthesized nanocatalyst (Fig. 2). Figure 3 displays the UV-vis diffuse reflectance spectra of Znpc-TiO_2 and TiO_2 recorded in the range of 200–800 nm. In addition to the fundamental absorption band of TiO_2, it showed a lower reflection in the range of 500-780 nm, corresponding to zinc phthalocyanine. The band gaps of the samples were calculated by plotting $(\alpha h\nu)^{1/n}$ (α = abs. coeff., $E = h\nu = hc/\lambda$ = 1242.376 /wavelength (nm), n = 1/2, 2 for direct and indirect transitions) against the energy. The reflectance data were converted to absorption according to the Kubelka-Munk (K-M) theory. The exact band gap of the samples was estimated by Tauc plot. The estimated band gap energy for the Znpc and undoped TiO_2 are 1.6 and 3.2 eV respectively and can be seen in the inset of Fig. 3. Znpc-TiO_2 could be more active due to the presence of both Znpc and TiO_2 as compared to

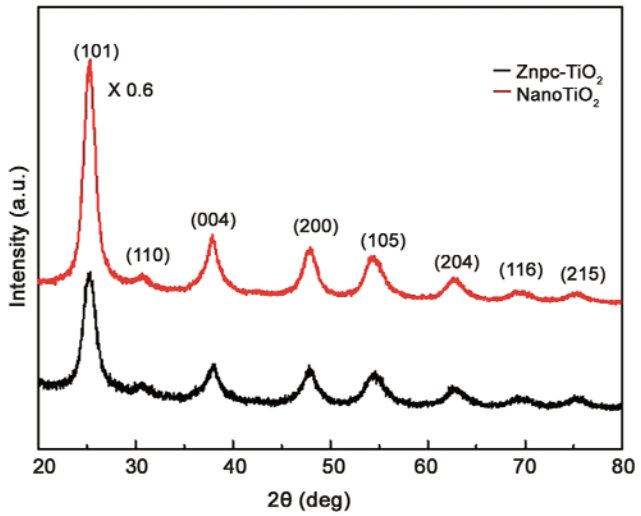

Fig. 1 — XRD of Znpc-TiO_2 and TiO_2 nanocatalysts.

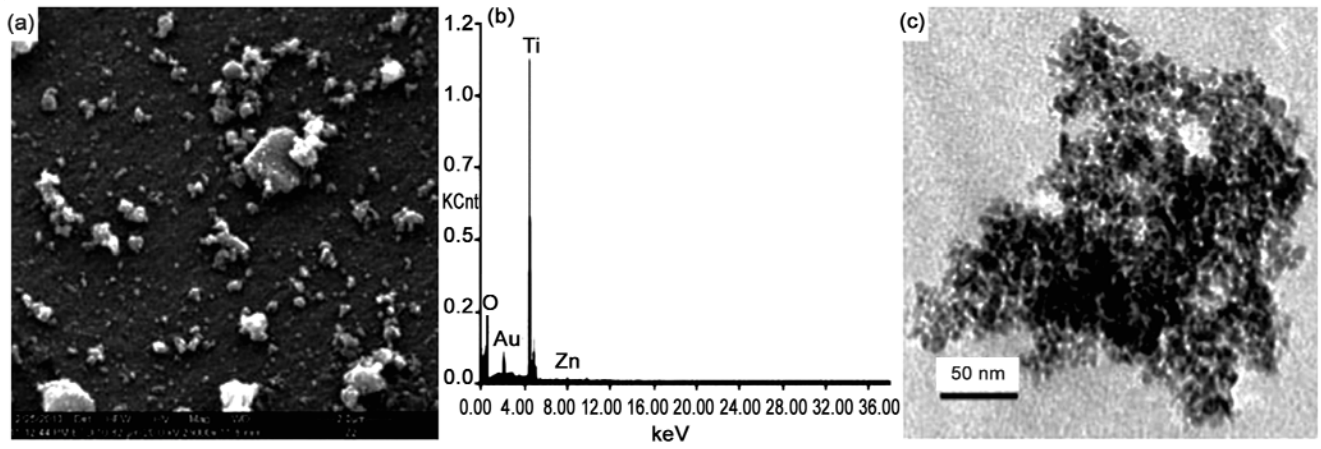

Fig. 2 — (a) SEM, (b) EDX, and, (c) TEM image of Znpc-TiO_2 nanocatalysts.

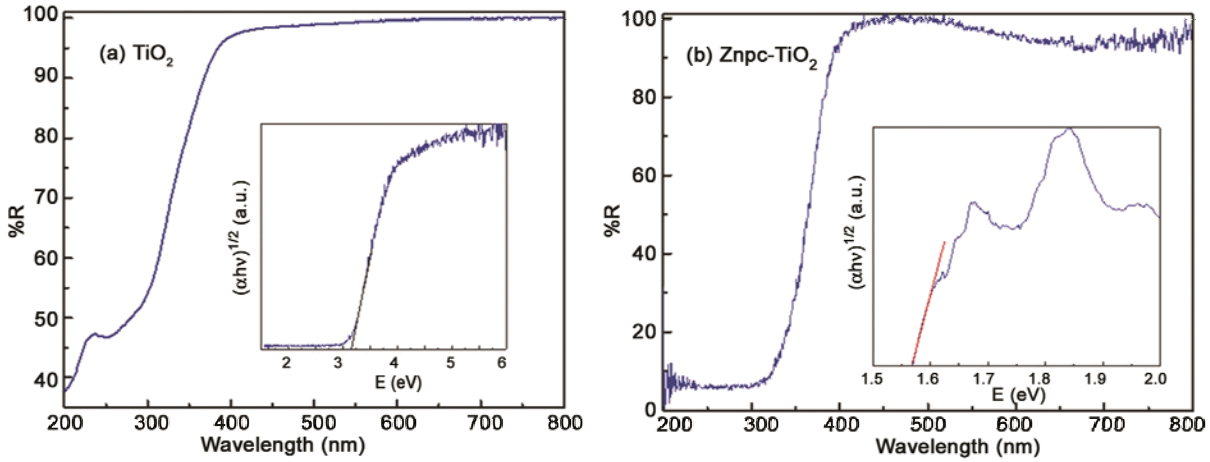

Fig. 3 — UV-vis-DRS of (a) TiO_2, and (b) Znpc-TiO_2 catalysts. [Inset: Tauc plots].

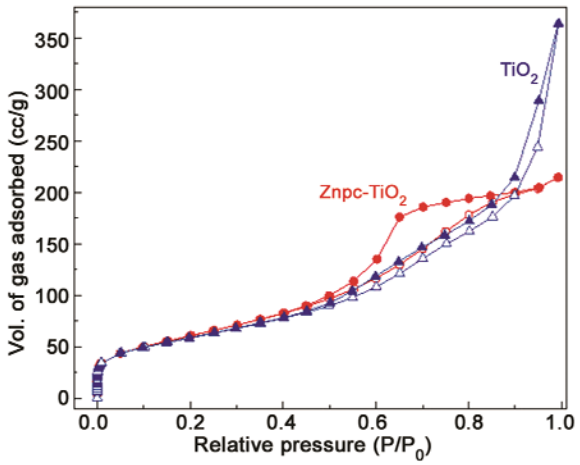

Fig. 4 — Nitrogen sorption isotherm of nano TiO_2 and Znpc-TiO_2.

TiO_2 alone. Figure 4 shows the N_2 sorption isotherms of Znpc-TiO_2 measured at 77 K. The N_2 sorption isotherms show hysteresis at P/P_0 = 0.4-0.45, indicating the presence of mesopores. Furthermore, there was sharp uptake at very low pressure range which may be attributed to monolayer deposition or the presence of the microporosity. The surface areas calculated from the BET (SA_{BET}) and Langmuir (SA_{Lang}) equations were 247 and 385 $m^2\ g^{-1}$ for Znpc-TiO_2, respectively. Figure 5 shows the XPS survey spectra and fitted spectra of Ti, O and Zn, depicting the presence of Znpc and TiO_2. All physico-chemical characterizations supports the co-existence of both Znpc and TiO_2 in the Znpc-TiO_2 catalysts.

Photocatalytic degradation of sulfur mustard

Blank experiments were performed to prove the photocatalytic degradation of SM. Only light (photolytic degradation) could not degrade SM effectively. This observation is in accord with the earlier reports.[11,18] Another blank experiment was also performed in the absence of light and in presence of catalyst. It resulted in 97% SM degradation in 20 h. The degradation can be ascribed to high surface area and the existence of reactive functional groups. In absence of light, SM molecule was found to be degraded into elimination and hydrolysis products. Interestingly, in presence of light and Znpc-TiO_2 catalyst the SM molecule was found to be degraded completely within as quickly as 60 min as can be seen in Fig. 6. However, in the case of undoped TiO_2, within 60 min only 50% SM degradation was observed; complete degradation required 6 h. The additive effect of Znpc and TiO_2 make Znpc-TiO_2 an effective photocatalyst towards degradation of SM. Photocatalytic degradation of SM molecule on Znpc-TiO_2 results into various products like oxidation, elimination, hydrolysis and rearranged products which were observed by GC-MS and are consistent with earlier reports [19]. SM disulfide was one of the products formed majorly upon cleavage of C-S bond. The amount of SM disulfide increased initially to 980 ppm and thereafter decreased with increase in time. The decreasing trend of SM disulfide with time can be attributed to its degradation to CO_2, HCl, H_2SO_4 and H_2O.

Upon illumination with sunlight both Znpc and TiO_2 were activated. TiO_2 absorbs UV and excites an electron from the VB to CB leaving a positive hole. Electron reacts with oxygen and form superoxide anion radical, while the hole reacts with hydroxyl ions to form hydroxyl radicals. Superoxide anion radicals accepts proton to form hydroperoxide radical ($O_2H^{\bullet}$). Hydroxyl radical upon dimerization will form H_2O_2. Znpc upon visible light absorption excites an electron from HOMO to LUMO and generates the Znpc cation radical ($dye^{\bullet+}$),

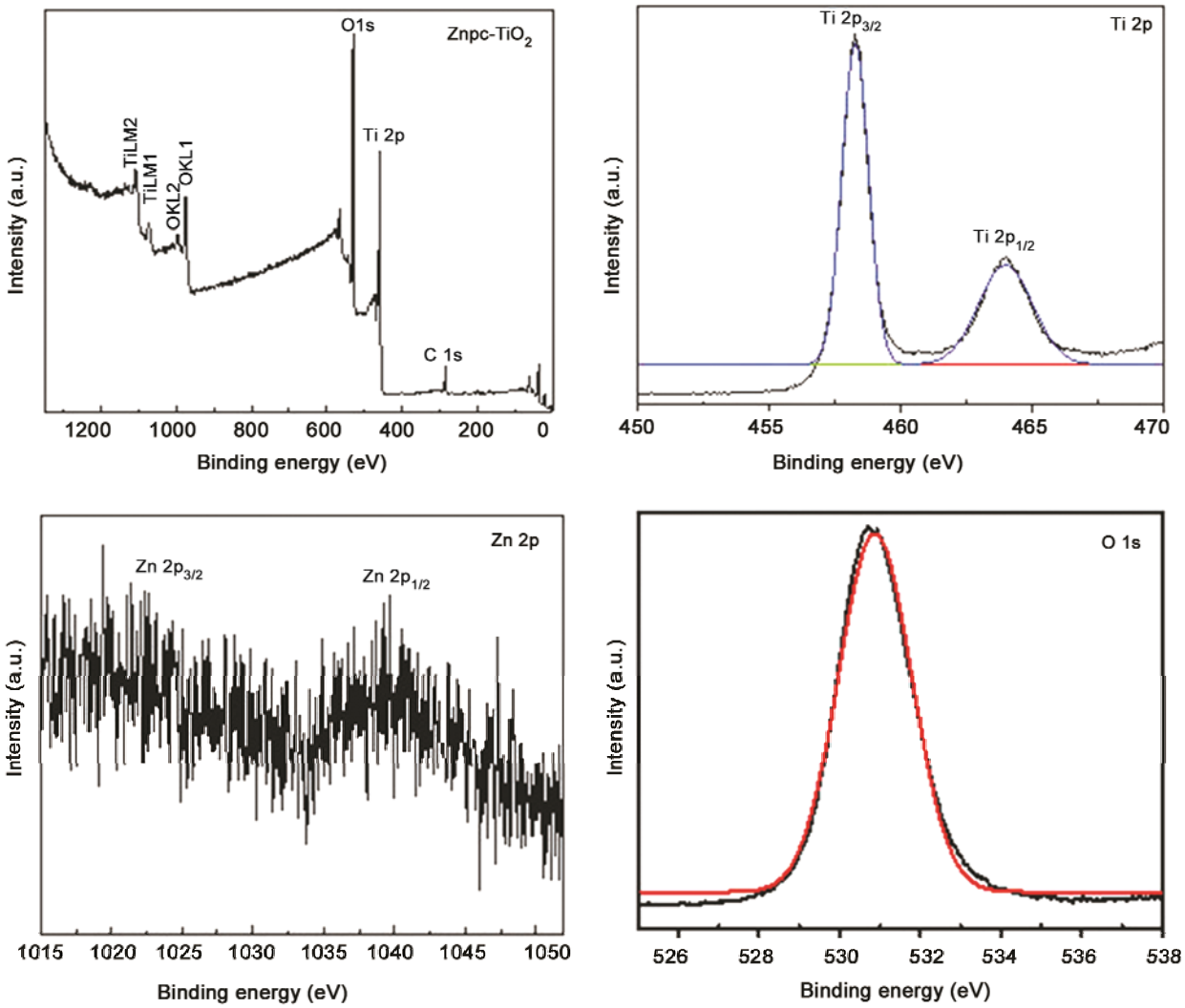

Fig. 5 — XPS survey and fitted spectra of Znpc-TiO_2.

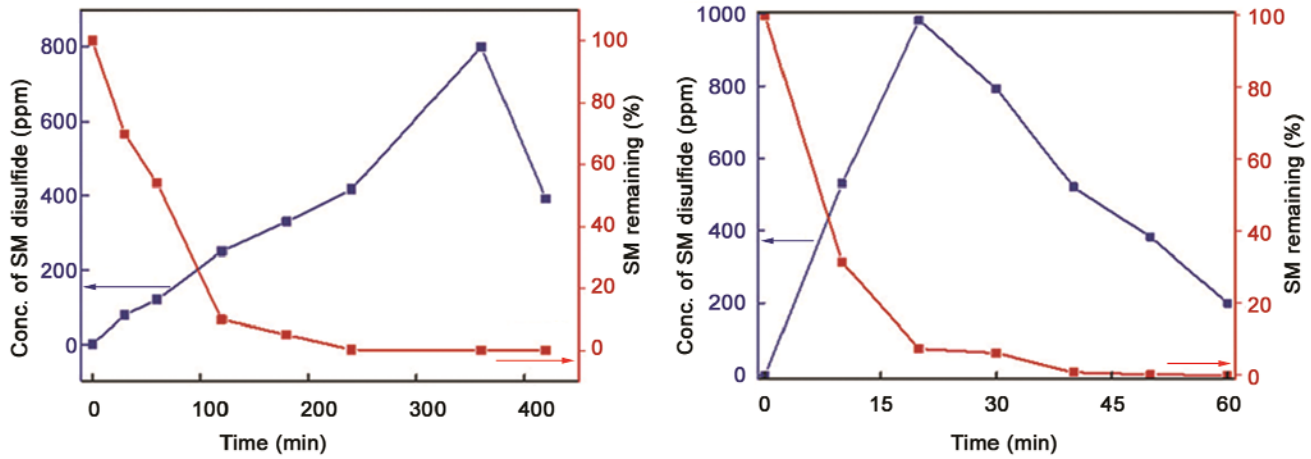

Fig. 6 — SM degradation pattern on (a) TiO_2, and, (b) Znpc-TiO_2 nanocatalysts.

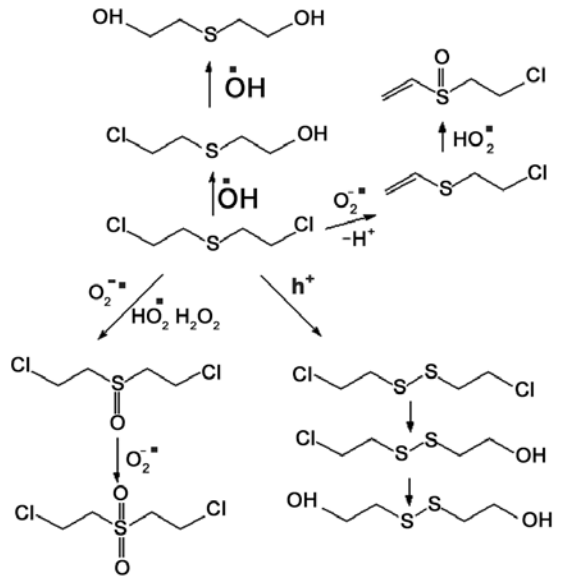

Photocatalytic degradation of SM on Znpc-TiO_2

Scheme 1

and the excited charge is then injected into the CB of TiO_2. Znpc also generates $^1O_2$ via energy transfer. All the reactive species react with SM molecule and form various products include hydrolysis, elimination, oxidation, and rearranged products (Scheme 1). This mechanism was found to be similar and consistent with earlier reports.[11,13,17,19] Irrespective of the dye, dye sensitized TiO_2 follows the same mechanism towards the degradation of pollutants. Znpc-TiO_2 catalyst shows efficient degradation within 60 min as compared to ZnO, Mn_2O_3, undoped TiO_2, M-TiO_2, N-TiO_2, S-TiO_2 and Fepc-TiO_2 (Table 1).[13,17,19]

Photocatalytic degradation of MG dye

For studying the photocatalytic degradation of MG, 3.0 mL of the supernatant solution was taken and absorbance was measured spectrophotometrically at λ_{max} = 620 nm. The absorbance of the solution was found to decrease with increasing time, i.e., concentration of dye decreased with time. The degradation reaction was well fitted into first order kinetics. The rate constant was determined by using the expression, k = 2.303×slope. Initially, the degradation was very fast, then it became slow. Photocatalytic degradation of the MG dye with time is depicted in Fig. 7, as the decrease in relative concentration of dye with the time of irradiation. A clear solution was observed indicating complete degradation of MG dye. The rate of reaction was found to increase on increasing the amount of Znpc-TiO_2.

Table 1 – Photocatalytic degradation of SM on various catalysts

Catalyst	Degrad. time (min)	Ref.
Polyoxometalates embedded in titania nanoparticles	90	11b
M/TiO_2/SiO_2 (M=V, Fe, Mn)	120	11c
N,S-TiO_2	180	13b
V-TiO_2	180	13c
ZnO	720	13d
S-TiO2	120	13e
Mn_2O_3 nanobelts	480	13f
Nano TiO_2	240	17
Fepc-TiO_2	70	19
Znpc-TiO_2	60	This study

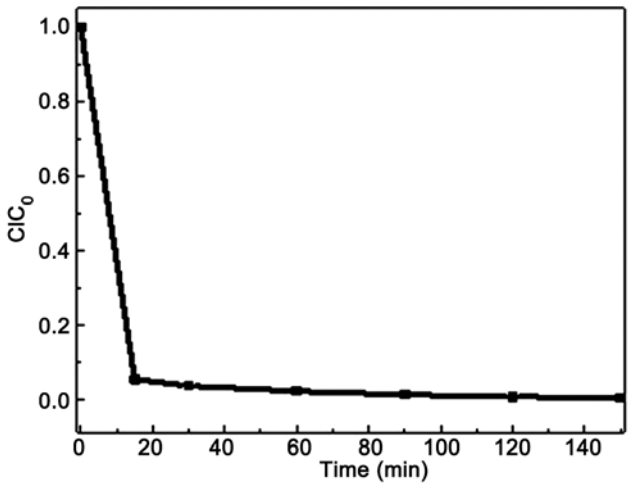

Fig. 7 – Effect of time on photocatalytic degradation on MG dye. [Znpc-TiO_2:25mg; MG: 50 ppm].

The % of dye degradation increased upon increasing the amount of catalyst. As the amount of catalyst increased, the exposed surface area was also increased due to increased active sites of the photocatalyst. In typical textile effluents, the dye concentration ranges from 0.15 to 0.2 g L^{-1}. The effect of the degradation rate was determined by varying the initial concentration from 0.02 to 0.1 g L^{-1} at constant catalyst loading (0.025 g L^{-1}, pH 7). Further, the dye concentration inversely affects degradation efficiency. As the dye concentration increases, the equilibrium adsorption of dye on the catalyst surface active sites increases, which decreases the competitive adsorption of hydroxyl radicals on the same sites. This decreases the formation rate of hydroxyl radicals which plays a major role in the degradation efficiency. Another reason for the observed

low degradation rate is the lower photon adsorption on catalyst. With the increase in the initial dye concentration, the chance of the photons entering into the solution decreases. Upon absorption of desired wavelength, an electron will be excited to the singlet state in MG dye. Then it undergoes intersystem crossing (ISC) to form the more stable triplet state. In addition, on absorption of the same irradiation, the photocatalyst excites an electron from valence band to conduction band. The electron reacts with adsorbed oxygen to form superoxide anion radical. Holes present in the valence band abstract an electron from hydroxyl ion to form the $^{\bullet}OH$ radical. These highly reactive photogenerated species (superoxide anion radical, hydroxyl radicals) oxidize the dye and degrade it. According to the literature, the $^{\bullet}OH$ radical contributed mainly to the degradation of MG dye.

Conclusions

Zinc phathalocyanine (Znpc) immobilized TiO_2 nanocatalysts was synthesised as a new photoactive material. Photocatalytic degradation of sulfur mustard and malachite green dye was explored under sunlight irradiation. Complete detoxification of SM molecule and MG dye by Znpc-TiO_2 was observed within 60 min irradiation, while with undoped TiO_2 almost six times (360 min) longer irradiation time was required. SM and MG dye were found to be degraded into nontoxic intermediates and finally into SO_2, CO_2 and H_2O. Thus, the degradation of highly harmful compounds like SM and MG dye under natural sunlight by the Znpc-TiO_2 catalyst makes this material important for various detoxification applications in environmental as well as water purification. It also has potential for use in dye sensitized solar cells.

References

1 a) Pelaez M, Nolan N T, Pillai S C, Seery M K, Falaras P, Kontos A G, Dunlop P S M, Hamilton J W J, Byrne J A, O'Shea K, Entezari M H & Dionysiou D D, *Appl Catal B: Environ,* 125 (2012) 331; b) Zhou W J, Leng Y H, Hou D M, Li H D, Li L G, Li G Q, Liu H & Chen S W, *Nanoscale*, 6 (2014) 4698; c) Zhou W, Yin Z, Du Y, Huang X, Zeng Z, Fan Z, Liu H, Wang J & Zhang H, *Small*, 9 (2013) 140; d) Zhou W, Liu H, Wang J, Liu D, Du G & Cui J, *ACS Appl Mater Inter,* 2 (2010) 2385.

2 Zhang Z, Wang W, Jiang D & Xu J, *Catal Comm,* 55 (2014) 15.

3 Fang Y, Li Z, Yang B, Xu S, Hu X, Liu Q, Han D & Lu D, *J Phys Chem C*, 118 (2014) 16113.

4 Lin C, Song Y, Cao L X & Chen S W, *Nanoscale*, 5 (2013) 4986.

5 a) Vargas E, Vargas R & Núnez O, *Appl Catal B: Environ,* 156 (2014) 8; b) Hu M, Xu Y & Xiong Z, Chem Lett, 33 (2004) 1092; c) Maria C, Rosa D & Robert C, *Coord Chem Rev*, 233 (2002) 351; d) Ni M, Leung M K H, Leung D Y C & Samathy L K A, *Renewable Sustainable Energy Rev,* 11 (2007) 401.

6 Maeda K, Sahara G, Eguchi M & Ishitani O, *ACS Catal,* 5 (2015) 1700.

7 a) Thandu M, Comuzzi C & Goi D, *Internat J Photo energy,* 2015, Article ID 521367, http://dx doi org/10 1155/2015/521367; b) Wang Z, Mao W, Chen H, Zhang F, Fan X & Qian G, Catal Comm, 7 (2006) 518; c) Buddee S, Wongnawa S, Sriprang P & Sriwong C, *J Nanopart Res,* 16 (2014) 1.

8 Ismail A A & Bahnemann D W, *J Mater Chem,* 21 (2011) 11686.

9 Wang Q Q, Lin B Z, Xu B H, Li X L, Chen Z J & Pian X T, *Micropor Mesopor Mater,* 130 (2010) 344.

10 Kim K, Tsay O G, Atwood D A & Churchill D G, *Chem Rev,* 111 (2011) 5345.

11 a) Zuo G M, Cheng Z X, Li G W, Wang L Y & Miao T, *Environ Sci Technol,* 39, (2005) 8742; b) Naseri M T, Sarabadani M, Ashrafi D, Saeidian H & Babri M, *Environ Sci Pollut Res,* 20 (2013) 907; c) Neatu S, Parvulescu V I, Epure G, Petrea N, Şomoghi V, Ricchiardi G, Bordiga S, Zecchina A, *Appl Catal B: Environ*, 91(1-2), (2009) 546.

12 Bromberg L, Pomerantz N, Schreuder-Gibson H & Hatton T A, *Ind Eng Chem Res,* 53 (2014) 18761.

13 a) Ramacharyulu P V R K, Prasad G K, Kumar J P & Dwivedi K, *J Sci Ind Res,* 73 (2014) 308; b) Ramacharyulu P V R K, Nimbalkar D B, Praveen Kumar J, Prasad G K & Ke S-C, *RSC Adv,* 5 (2015) 37096; c) Ramacharyulu P V R K, Kumar J P, Prasad G K, Singh B, Sreedhar B & Dwivedi K, *J Mol Catal A: Chem,* 387 (2014) 38; d) Prasad G K Ramacharyulu P V R K, Singh B, Batra K, Srivastava A R, Ganesan K, Vijayaraghavan R, *J Mol Catal A: Chem,* 349 (2011) 55; e) Ramacharyulu P V R K, Kumar J P, Prasad G K & Sreedhar B, *Mater Chem Phy,* 148 (2014) 692; f) Ramacharyulu P V R K, Prasad G K, Kumar J P, Ganesan K, Singh B & Dwivedi K, *Environ Prog Sust Energy,* 32 (2013) 1118; g) Ramacharyulu P V R K, Kumar J P, Prasad G K & Srivastava A R, *Adv Por Mater,* 1 (2013) 397.

14 Arcibar-Orozco J A & Bandosz T J, *J Mater Chem: A*, 3 (2015) 220.

15 Baran W, Makowske A & Wardas W, *Dyes Pigm*, 76 (2008) 226.

16 Zhang G, Kim G & Cho W, *Energy Environ Sci,* 7 (2014) 954.

17 Ramacharyulu P V R K, Prasad G K, Ganesan K & Singh B, *J Mol Catal A: Chem,* 353-354 (2012) 132.

18 Cojocaru B, Parvulescu V, Preda E, Pure G, Somoghi V, Carbonell E, Salvaro M & Garcia H, *Environ Sci Technol,* 42 (2008) 4908.

19 Ramacharyulu P V R K, Muhammad R, Kumar J P, Prasad G K & Mohanty P, *Phys Chem Chem Phys,* 17 (2015) 26456.

20 Srivastava S, Sinha R & Roy D, *Aquat Toxicol,* 66 (2004) 319.

21 a) Sayilkan F, Asilturk M, Tatar P, Kiraz N, Arpac E & Sayilkan H, *J Hazard Mater,* 148 (2007) 735; b) Chen C C, Lu C S, Chung Y C & Jan J L, *J Hazard Mater,* 141 (2007) 520; c) Pare B, Sarwan B & Jonnalagadda S B, *Appl Surf Sci,* 258 (2011) 247; d) Liu Y, Ohko Y, Zhang R, Yang Y & Zhang Z, *J Hazard Mater,* 184 (2010) 386; e) Prado A G S & Costa L L, *J Hazard Mater,* 169 (2009) 297; f) Saikia L, Bhuyan D, Saikia M, Malakar B, Dutta D K & Sengupta P, *Appl Catal A: Gen,* 490 (2015) 42; g) Pathania D, Katwal R, Sharma G, Naushad M, Rizwan Khan M & Al-Muhtaseb A-H, *Inter J Biol Macromol,* 87 (2016) 366.

22 Chowdhury P, Moreira J, Goma H & Ray A K, *Ind Eng Chem Res,* 51 (2012) 4523.